Proceedings of the 37th International & 4th National conference on Fluid Mechanics and Fluid Power

FMFP2010

December 16-18, 2010, IIT Madras, Chennai, India

FMFP2010_____

THE TRANSITION FROM ADVECTION TO DIFFUSION IN CONVECTION ACROSS A HORIZONTAL PERMEABLE MEMBRANE

G. V. Rama Reddy,
BHEL Corporate R & D,
Vikas nagar, Hyderabad,
Andhra Pradesh, India.
E-mail: gvramareddy@gmail.com

B. A. Puthenveettil,
Dept. of Applied Mechanics,
IIT Madras, Chennai,
Tamil Nadu, India.
E-mail: apbraj@iitm.ac.in

ABSTRACT

We study convection driven by an unstable concentration difference across a horizontal permeable membrane due to a layer of brine lying over a layer of water across the membrane. The flow through the membrane changes the phenomena drastically from those in Rayleigh Benard convection; different regimes of convection across the membrane are observed [5]. By using a coarser membrane compared to that by [5], we find a new regime of convection where the Sherwood number scales linearly with the Rayleigh number. The planform plume-structure in this regime is presented. Phenomenology proposed is able to explain the flux scaling in the new regime.

KEYWORDS: High Rayleigh number convection, Wall normal blowing, Sheet plumes, Natural convection boundary layers. Flow through permeable membranes.

1. INTRODUCTION

When a permeable membrane separates a heavier miscible fluid above it from a lighter fluid below, based on the unstable density difference across the membrane that keeps decreasing with time, various regimes of convection could be set up. At large concentration differences, the transport across the membrane will be due to advection [5] while diffusion across the membrane will be predominant at lower concentration differences [4]. In all the cases, unstable lighter layers of fluid above and below the membrane cause turbulent convection away from the membrane; the arrangement could thus be used to study the effect of wall-normal advection or diffusion on turbulent convection. In addition to the importance of understanding the phenomenology of such a system, the effects encountered in such a configuration are of considerable practical interest in filtration, dialysis and biological systems where the effect of unstable concentration boundary layers on the transport

across membranes is still unclear ([2],[6]).

The dimensionless parameters that characterize concentration driven convection across the membrane are the Rayleigh number, $Ra= g\beta\Delta CH^3/\nu D$, the Schmidt number ($Sc=\nu/D$) and the aspect ratio, L/H. Here, g = the acceleration due to gravity, β = the coefficient of salinity, ΔC = the concentration difference between the bulk fluid on both sides of the membrane, H = height of the fluid layer, ν = the kinematic viscosity, D = the species diffusivity and L = the horizontal dimension of the fluid layer.

Puthenveettil and Arakeri, 2008 (hereinafter referred to as PA) conducted experiments using brine solution above water, separated by a membrane of pore size P_s=35µm and open area factor Γ=0.25. For $Ra>3.5x10^{11}$, advection dominated the transport across the membrane; advection was generated by the unstable system itself. Unstable liquid layers near the membrane give rise to the formation of sheet-plumes near the membrane surface. PA proposed that impingement of the large scale flow on the membrane results in a plume-free area on the membrane, and these unstable boundary layers to be present only on the opposite side of impingement of the large-scale flow, with no concentration drop across the membrane (Fig. 1(a)). The nature of these near-membrane boundary layers and the scaling of flux are changed from that in pure Rayleigh-Benard Convection (RBC) due to the advection across the membrane. The observed flux scaling $q\sim\Delta C^3$ was explained by assuming that the large-scale flow, having the strength of the Deardorff velocity scale (Deardorff, 1970), $W_* = (g\beta qH)^{1/3}$ drives a flow through the membrane which obeys Darcy's law, to obtain $Sh \propto Ra^2/Sc$. At lower concentrations ($Ra<7x10^{10}$), Sh scaled as $Ra_w^{1/3}$ when the Rayleigh number near the membrane, $Ra_w=g\beta\Delta C_w H^3/\nu\alpha$ was based on ΔC_w above or below the membrane (fig.1 (b)); the details are discussed in Puthenveettil and Arakeri, 2005.

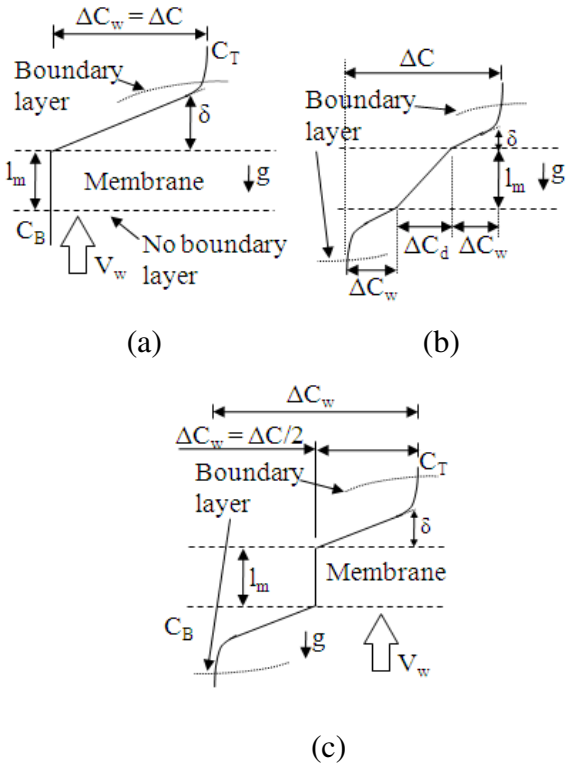

Fig.1: Concentration profiles across the membrane pore observed by PA. (a), The advection regime; (b), the diffusion regime; (c), the combined regime.

In between these two regimes, PA observed a regime, which they termed as the combined regime, with an inferred concentration profile as shown in fig.1(c), where $Sh\sim Ra_w^{1/3}$ when $\Delta C_w=\Delta C/2$. As shown in their Fig. 15(a), both sides of the membrane were covered with plumes in this regime. It is intriguing that the advection dominated concentration profile would change over to that of diffusion dominated without having a regime where advection balances diffusion. In this paper, by using a membrane that is coarser, but also thicker than that in PA we extend the

range of Ra over which this transition from advection to diffusion occurs inside the membrane.

We study turbulent natural convection caused by brine lying over a horizontal micro porous membrane with distilled water below it. Based on the pattern of near-membrane plumes and the scaling of flux with Ra_w, we classify the regimes of convection observed in the present experiments. We find a new regime of convection where advection balances diffusion in the membrane pore, and explain the physics behind the flux scaling in this new regime by a phenomenology.

2. EXPERIMENTAL SET-UP AND MEASUREMENTS

2.1 Set-up

A schematic of the experimental set-up is shown in Fig. 2. Since the set-up is similar to that in PA with the difference that the membrane used in the present study is coarser (P_s=45.6μm and Γ=0.31) and thicker (l_m=72.5μm), we briefly summarize the relevant details of the set-up; the reader is referred to PA and Rama Reddy, 2009 for further details. The zoomed view of the membrane is shown in fig. 2. NaCl solution is used as the top tank solution and distilled water with Rhodamine-6G dye (0.96 P.P.M) as the bottom tank solution. The inner cross-section of the each tank is 0.15x0.15 m^2 and height of the fluid layer is 0.236 m. In present study, we use three starting concentrations of the salt solution viz. 10 g/l and 8 g/l. A typical experiment runs approximately for 2.5 days.

2.2 Diagnostics and measurements

The plumes are visualized using a Nd:Yag pulsed laser (532 nm, 100 mJ/pulse and 50 Hz.). Since $(\Delta\rho/\rho)|_{dye} << (\Delta\rho/\rho)|_{salt}$, and $Sc_{dye} >> Sc_{salt}$ (2000>600), the dye acts as a passive scalar, following the convection and

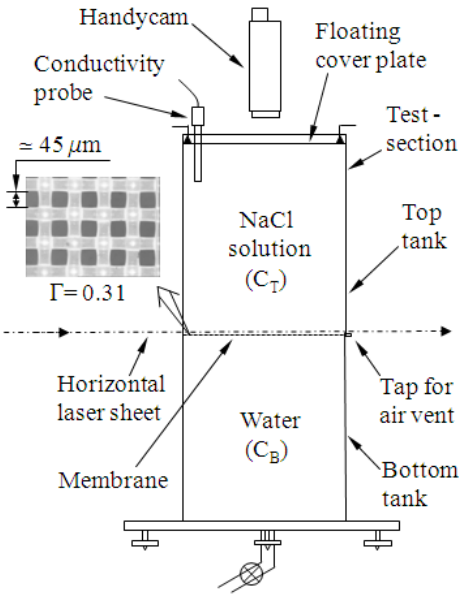

Fig.2: Schematic of the experimental set-up with the microscopic view (100X) of the membrane used in the present experiments.

diffusion patterns of the salt solution. The changing concentration of salt in the top tank solution is estimated from the transient measurements of electrical conductivity of the top tank solution by a 4-pole, platinized conductivity probe. The conductivity data is acquired at a frequency of 1.56 Hz.

2.3 Calculation of flux and density potential

The solution in both the tanks away from the membrane is assumed to be well mixed; this assumption is generally true for turbulent convection with these boundary layers and well mixed bulk. The measured conductivity data of the salt solution is converted to its concentration using the standard relation from Lide, 2003. Using mass conservation of the solutions in the two tanks at any instant, the instantaneous driving potential can be written as $\Delta C(t)=2C_T(t) - C_T^0$, where superscript 0 indicates the value before the start of

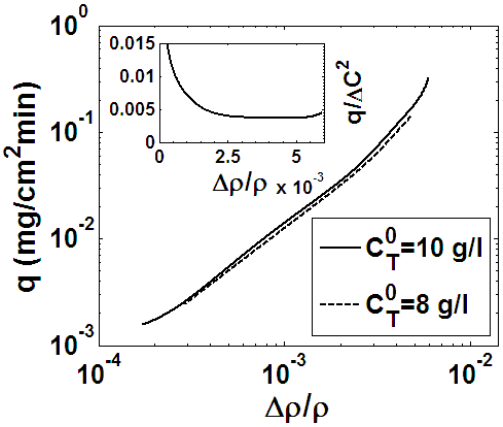

Fig. 3: Variation of the flux with the normalized density difference $\Delta\rho/\rho$. The inset shows that $q \sim \Delta C^2$ for $2.5\text{x}10^{-3} \leq (\Delta\rho/\rho) \leq 5.1\text{x}10^{-3}$.

the experiment. From the conservation of mass in the top tank, the flux of salt across the membrane,

$$q = -H\frac{dC_T}{dt}, \qquad (1)$$

where t is time. As differentiation of the raw concentration data with time results in large fluctuations, we fit a fourth order exponential decay curve. Since the solution to the theoretical concentration C(t) is exponential for a constant V_w in the membrane pore, we use an exponential fit in the experiments. However, the advection velocity V_w reduces with time in the experiments.

Even though the present experiments are unsteady, the present system can be shown to be steady by understanding the relevant time scales in the system. Even at the start of the experiment, where the flux is changing at its fastest rate, since the ratio of time scale of decrease of salt t_q ($\sim \frac{q}{dq/dt}$) and the time scale of one large-scale circulation t_{W_*} ($\sim \frac{H}{W_*}$) is very high ($\simeq$70), many large-scale circulations will observe a constant flux over a time period or to their lifetimes. As other time scales in the system are even smaller than t_{W*}, the convection is hence quasi-steady, and the present experimental results can be compared with steady RBC.

3. SCALING OF FLUX

During the course of the experiment, mixing of the solutions in the two tanks occurs, and ΔC across the membrane and hence the net transport of salt, decreases with time. Figure 3 shows the dependence of the flux of salt, q on the normalized density difference ($\Delta\rho/\rho=\beta\Delta C$) for experiments started with C_T^0 = 10g/l and 8g/l. Lower C_T^0 experiments are conducted to visualize the plume structure during the later period of the experiments, since mixing reduces the contrast of the plume-structure of the planform images. The slope of the curve for the experiment with C_T^0=10 g/l, changes thrice at $\Delta\rho/\rho = 5.1\text{x}10^{-3}$, $2.5\text{x}10^{-3}$ and $0.71\text{x}10^{-3}$ indicating four different regimes of convection. Figure 4 shows the flux in dimensionless form, Sh plotted against the Rayleigh number. The changes of regime seen in fig. 3 could be observed at $Ra=4.96\text{x}10^{11}$, $2.43\text{x}10^{11}$ and $0.69\text{x}10^{11}$ in fig. 4.

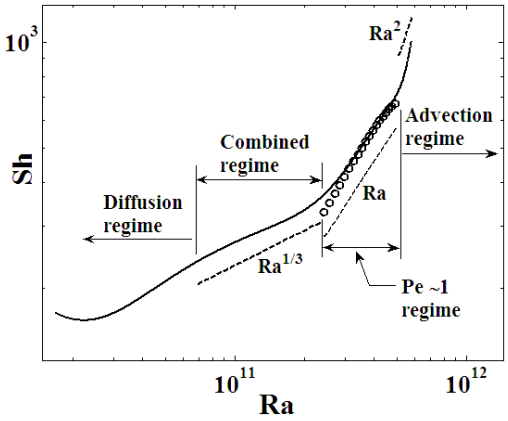

Fig. 4: Variation of Sherwood number against the Rayleigh number.

In the first regime, for $\Delta\rho/\rho > 5.1\text{x}10^{-3}$, the flux scales as $q \sim \Delta C^3$ or $Sh \sim Ra^2$ as shown in fig. 4. The flux scaling of $Sh \sim Ra^2$ and the planforms observed in this regime are similar to those

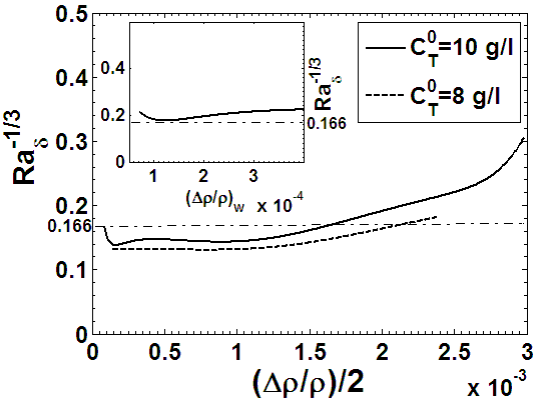

Fig.5: Variation of $Ra_\delta^{-1/3}$ with $\frac{1}{2}(\Delta\rho/\rho)$.

observed by PA in their advection regime. However, the agreement of the present data with the Ra^2 scaling seems to be approximate as the range of this regime is less and the data seems to be influenced by the initial perturbation in filling the top tank. The focus of this paper is however not on this regime as this regime has been explored thoroughly by PA.

The regimes below $Ra=2.43x10^{11}$ could also be shown to be same as those observed by PA, by expressing the flux normalized by the near-membrane scales as

$$Ra_\delta^{1/3} = \frac{q}{D\Delta C Z_w/H} \qquad (2)$$

Here, Ra_δ is the Rayleigh number based on ΔC_w and the diffusion layer thickness $\delta=D\Delta C_w/q$, and $Z_w=(\nu D/g\beta\Delta C_w)^{1/3}$ is a near-membrane length scale for turbulent natural convection proposed by Theerthan and Arakeri, 2000. $\Delta C_w=\Delta C$ in the advection regime (fig.1(a)). $\Delta C_w=\Delta C/2$ in the combined regime (fig1.(c)) and $\Delta C_w=(\Delta C-\Delta C_d)/2$ in the diffusion regime (fig.1(b)). In all subsequent analyses, the effective Rayleigh number, Ra_w in any regime is based on the corresponding ΔC_w in that regime. $Ra_\delta^{-1/3}=0.166$ if the boundary layers above the membrane maintain their character same as those

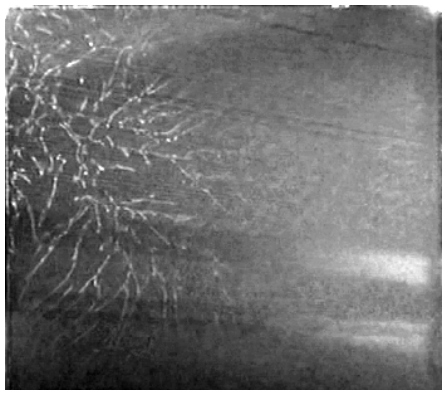

Fig.6: Planform of the near-membrane sheet-plumes (the white lines) at the start of the Pe~1 regime ($Ra_w=4.56x10^{11}$) obtained from the experiment with C_T^0=8 g/l showed in fig. 3.

in RBC. Variation in near-membrane phenomena would be reflected strongly in the variation of $Ra_\delta^{-1/3}$ as $Ra_\delta^{-1/3}$ is defined purely based on the near-membrane variables. If we use $\Delta C_w=\Delta C/2$ in eq. (2), the variation of $Ra_\delta^{-1/3}$ with $\frac{1}{2}(\Delta\rho/\rho)$ is as shown in Fig. 5. For $3.5x10^{-4} < \frac{1}{2}(\Delta\rho/\rho) < 1.25x10^{-3}$ ($6.9x10^{10} < Ra < 2.43x10^{11}$ in fig. 4) the non-dimensional flux is constant and is approximately equal to the magnitude of the flux in RBC, similar to that in fig. (7)(b) in PA in their combined regime. The inset of fig. 5 shows that $Ra_\delta^{-1/3}$, corrected for diffusion drop across the membrane $\Delta C_d = ql_m/\Gamma D$, is approximately equal to that of RBC for $(\Delta\rho/\rho)_w < 2.7x10^{-4}$ ($Ra<6.9x10^{10}$ in fig. 4). Hence, the transport of salt through the membrane in this regime is entirely due to diffusion, and the boundary layers in this regime are of diffusion type as those in RBC. We do not discuss these combined and diffusion dominated regimes further as they have been discussed in detail by PA.

The new phenomena that is observed in our study is the presence of a regime for $2.43x10^{11} \leq Ra \leq$

$4.96x10^{11}$, where Sh~Ra (fig. 4); the inset of fig. 3 shows that $q \sim \Delta C^2$ in the corresponding $\Delta\rho/\rho$ range of $2.5x10^{-3} \leq (\Delta\rho/\rho) \leq 5.1x10^{-3}$. We call this regime the Pe~1 regime, for reasons that will become obvious later, and focus our attention on this regime further.

4. THE Pe~1 REGIME

The top view of the distribution of plumes at the beginning of this experiment is shown in Fig. 6. The alignment of plumes in this regime, even in the central region of the membrane, is relatively less compared to that in the advection regime (see fig. 8(a) in PA). It is known that the main effect of large-scale flow is to align the near-membrane plumes along the direction of the near-membrane shear ([5],[8]). This lower alignment of plumes in the new regime implies a lower strength of large-scale flow and hence a weaker through-flow (indicated in Fig. 8) compared to those in the advection regime. The strength of the large-scale flow W_* ($=0.34x10^{-2}$ m/s at $Ra_w=4.56x10^{11}$) in the Pe~1 regime is lesser than that in the advection regime of PA ($W_*= 0.51x10^{-2}$ m/s at $Ra_w=4.71x10^{11}$) owing to the lower flux. The vacant region in the planforms of this regime indicates that there is a through-flow and hence advective effects cannot be neglected in the membrane pore. If pure advection occurred, we would observe the advection regime identified by PA, and also seen at the beginning of our experiments. If pure diffusion occurred, the planform would totally be covered with plumes ([4],[5]). Hence, we anticipate that both advection and diffusion play a non-negligible role in the transport inside the membrane pore in this new regime.

The relevant parameter that decides the relative magnitude of

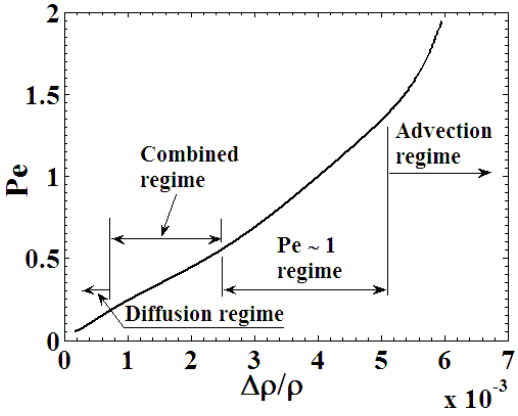

Fig.7: Variation of Peclet number with $\Delta\rho/\rho$ for the expt. with C_T^0=10g/l showed in fig. 3.

advection and diffusion inside the pore is the membrane Peclet number

$$Pe = V_w l_m/D, \qquad (3)$$

where V_w is the spatial average velocity of the fluid inside the membrane pore and l_m is the thickness of the membrane. Assuming that the mechanism that decides the value of V_w in the advection regime, namely the impingement of the large-scale flow, proposed in PA still holds in the new regime, we choose

$$V_w = f\frac{\kappa}{2\nu l_m \Gamma}(g\beta qH)^{2/3} \qquad (4)$$

given by PA. Here, f is a prefactor which is expected to be constant throughout the experiment. Since $V_w=2q/\Gamma\Delta C$ in the advection regime (PA), equating this V_w to that in eq. (4) we obtain f=1.64. The variation of Pe, calculated from eq. (4) for the C_T^0=10 g/l experiment in fig. 3(a), is shown in fig. 7. For the $\Delta\rho/\rho$ range of the new regime $2.5x10^{-3} \leq \Delta\rho/\rho \leq 5.1x10^{-3}$ ($2.43x10^{11} \leq Ra \leq 4.96x10^{11}$), Pe is of order 1; the advective and the diffusive effects are of the same order in the membrane pore in the new regime. We hence term this regime of convection as the Pe~1 regime, and based on the observation, we propose a phenomenology to explain the flux

scaling, $q \sim \Delta C^2$ in the following section.

4.1 Phenomenology of flux scaling in the Pe~1 regime

Consider the control volumes of the top and the bottom tanks shown in fig. 8. We denote the left half of the membrane as LH and the right half as RH considering the specific case of upward flow in LH and downward flow in RH. The phenomena are assumed to be symmetric with respect to the vertical centre line. The concentration profiles shown in fig. 8 are area averaged over LH and RH as the case might be. Let C_{L2} and C_{R2} be the concentration of the fluid on the membrane surface at $y=l_m$ in LH and RH respectively, while C_{L1} and C_{R1} the concentration at $y=0$ in LH and RH respectively. For the same V_w in LH and RH, symmetry implies

$$\left(\frac{\partial C}{\partial y}\right)_{\text{LH, lm}} = \left(\frac{\partial C}{\partial y}\right)_{\text{RH, 0}} = \xi_1 \qquad (5)$$

$$\left(\frac{\partial C}{\partial y}\right)_{\text{LH, 0}} = \left(\frac{\partial C}{\partial y}\right)_{\text{RH, lm}} = \xi_2 \qquad (6)$$

where C(y) is the concentration of NaCl in the membrane pore. As this regime is a transition regime between the advection and the diffusion regimes, we expect a non-linear concentration drop in the Pe~1 regime. Hence, we consider one dimensional convection-diffusion equation with constant V_w inside the membrane pore,

$$V_w \frac{\partial C}{\partial y} = D \frac{\partial^2 C}{\partial y^2} \qquad (7)$$

Solving equation (7) using equations (5) and (6) for LH, we get a condition to relate the concentration gradients on both sides of the membrane as $\xi_1=\xi_2 e^{Pe}$. This implies that the concentration gradient on the side of impingement of large-scale flow is less than that on the opposite side of the membrane by a factor of $1/e^{Pe}$. When Pe=0, as one would expect in the diffusive regime, the concentration gradient on both sides of the membrane become equal.

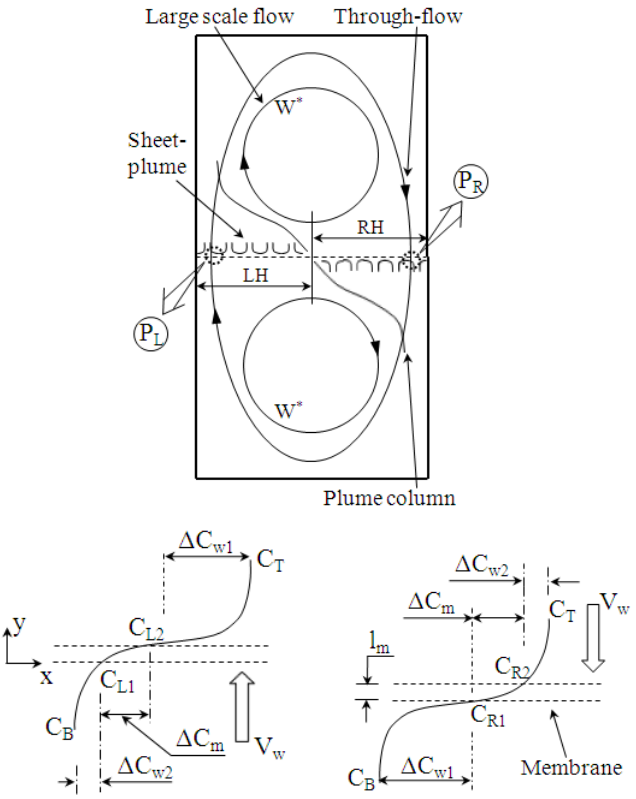

Fig.8: Schematic of flows in the test-section. Here P_L (left profile) and P_R are the zoomed views of the spatially averaged concentration profiles in the membrane pore on LH and RH of the membrane respectively.

From the mass balance in the top tank, we get

$$\forall_T \frac{\partial C_T}{\partial T} = \Gamma \frac{A}{2} V_W (C_{L2} - C_{R2}) - \Gamma \frac{A}{2} D(\xi_1 + \xi_2), \qquad (8)$$

where $\forall_T$ is the volume of the top tank and A is the cross sectional area of the membrane. From eqs. (7) and (8), the concentration gradient

$$\xi_1 = \frac{e^{Pe}}{1+e^{Pe}} \left(\frac{2q}{\Gamma V_W} - \Delta C_{wd}\right) \frac{V_W}{D} \qquad (9)$$

where $\Delta C_{wd}=\Delta C_{w1}-\Delta C_{w2}$. Solving eq. (7) using eqs. (6), (9) and the condition $\xi_1=\xi_2 e^{Pe}$, the concentration

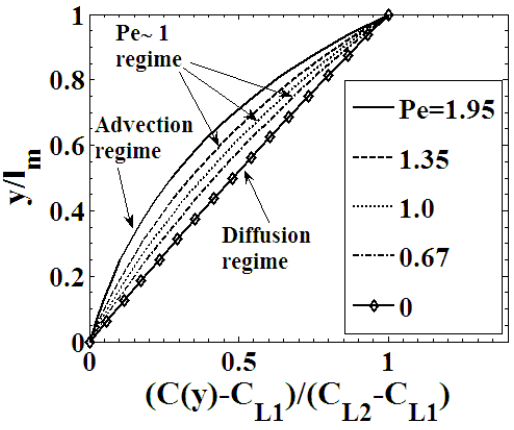

Fig.9: Dimensionless concentration distribution inside the membrane pores in different regimes.

distribution inside the membrane pore C(y) is obtained as

$$\frac{C(y)-C_{L1}}{\frac{2q}{\Gamma V_w}-\Delta C_{wd}} = \frac{e^{Pe_y}-1}{e^{Pe}+1} \qquad (10)$$

where $Pe_y=V_w y/D$. However, one still cannot calculate C(y) from eq. (10) as ΔC_{w2} and ΔC_{L1} are unknowns. Obtaining ΔC_{w2} from eq. (A3), as shown in detail in Appendix, the concentration drop across the membrane can be calculated by substituting $y=l_m$ in equation (10) as

$$\Delta C_m = \frac{e^{Pe}-1}{e^{Pe}+1}\left(\frac{2q}{\Gamma V_W} - \Delta C_{wd}\right) \qquad (11)$$

Note that eq. (11) is the general expression for the concentration drop across a permeable membrane for a given flux and V_w for all the regimes of convection. In the advection regime, $\frac{2q}{\Gamma V_w}=\Delta C$ [5] and $\Delta C_{wd}\rightarrow\Delta C$ so that $\Delta C_m\rightarrow 0$ when $Pe\rightarrow (2q/\Gamma\Delta C)/(D/l_m)$. In the diffusion regime, Lim $(V_w,\Delta C_{wd})\rightarrow 0$ $\Delta Cm=\frac{ql_m}{\Gamma D}$, the same expression obtained by PA in the diffusion regime. The concentration drop across the membrane increases from zero at the beginning of the Pe~1 regime till the end of the regime, showing the increasing effects of diffusion. Using eq. (11) and the condition $\Delta C_{w1}+\Delta C_{w2}+\Delta C_m=\Delta C$ obtained from fig. 6, we get the relevant driving potential above the membrane as

$$\Delta C_{w1} = \frac{\Delta C}{2} + \frac{q}{\Gamma V_w} D_1 + D_2 \Delta C_{wd} e^{Pe}, \quad \text{and} \qquad (12)$$

$$\Delta C_{w2} = \frac{\Delta C}{2} + \frac{q}{\Gamma V_w} D_1 - D_2 \Delta C_{wd} \qquad (13)$$

where $D_1=\frac{1-e^{Pe}}{1+e^{Pe}}$ and $D_2=\frac{1}{1+e^{Pe}}$. Note that ΔC_{w1} becomes ΔC, and ΔC_{w2} becomes zero, the condition that prevails in the advection regime when $Pe\rightarrow\frac{2q/\Gamma\Delta C}{D/lm}$. In the diffusion regime, $V_w\rightarrow 0$, as expected both ΔC_{w1} and ΔC_{w2} become equal to $(\Delta C-\Delta C_m)/2$. The dominance of the concentration drop ΔC_{w1} decreases as the experiment proceeds and becomes equal to ΔC_{w2} in the diffusion regime, at this time the entire area of the membrane is covered with plumes ([4],[5]). The above analysis is not valid in the combined regime, which is observed here as well as well as in PA. The additional physical mechanism, possibly plume suction that causes no concentration drop in the membrane in this regime, has not been considered in the above analysis.

Using eqs. (A3) and (13), C(y) in different regimes is calculated for the experiment with $C_T^0=10$ g/l in fig. 3, and shown in Fig. 9. The concentration gradient in the diffusion regime, as expected, is constant. Since the concentration in the membrane pore is expected to be constant in the advection regime when Pe=4, as shown by PA (their Fig. 16(a)), the concentration profile shows a substantial drop inside the membrane pore in the range of advection regime in the present experiments. This could be the reason for slight deviation from the Ra^2 scaling in the advection regime seen in fig. 4. Figure 9 clearly shows that the concentration profile in

the membrane pore in the Pe~1 regime is non-linear illustrating that both advection and diffusion are important inside the membrane pore in the present Pe~1 regime.

In order to understand the near-membrane phenomena in the Pe~1 regime, we observe the behavior of $Ra_\delta^{-1/3}$ with $\Delta\rho/\rho$ in the Pe~1 regime. As the flux q is from the entire area of the membrane where as ΔC_{w1} and ΔC_{w2} act on only some area, we plot $Ra_\delta^{-1/3}$ based on the behavior of net flux, q_d-q_u normalized by the appropriate equivalent concentration difference, ΔC_{w1}, where

$$q_d = \Gamma(V_w C_{R2} + D\xi_2) \qquad (14)$$

is the downward flux from RH of the membrane and

$$q_u = \Gamma(V_w C_{L2} + D\xi_1) \qquad (15)$$

is the upward flux from LH of the membrane. Here q_u is considered as inward flux and q_d as outward flux with reference to the upper surface of the membrane. If we express RHS of eq. (8) in terms of q_d and q_u and use $q=-HdC_T/dt$, we obtain $q_d-q_u=2q$. ΔC_{w1} is chosen for determining $Ra_\delta^{-1/3}$ as $\Delta C_{w2} < \Delta C_{w1}$ in the Pe~1 regime. Figure 10 shows the variation of $Ra_\delta^{-1/3}$ expressed as $\frac{q_d-q_u}{D\Delta C_{w1}/Z_{w1}}$, with $(\Delta\rho/\rho)_{w1}$. For $1.94\text{x}10^{-3} \le (\Delta\rho/\rho)_{w1} \le 4.89\text{x}10^{-3}$ (or $2.5\text{x}10^{-3} \le \Delta\rho/\rho \le 5.1\text{x}10^{-3}$), $Ra_\delta^{-1/3}$ is constant ($\simeq$0.166) implying that $q_d - q_u \sim \Delta C_{w1}^{4/3}$, similar to that in pure diffusion regime. However, since ΔC_{w1} is a function of V_w, through flow has an indirect effect in the flux scaling in this new regime. Based on this understanding, if we start the analysis with $Ra_\delta^{-1/3} = E(\Delta C)$, where $Ra_\delta^{-1/3}$ is based on q and ΔC_{w1}, then using ΔC_{wd} from eq. (A3), and eq. (12) for ΔC_{w1} in this expression, we get the flux scaling relation in the Pe~1 regime as

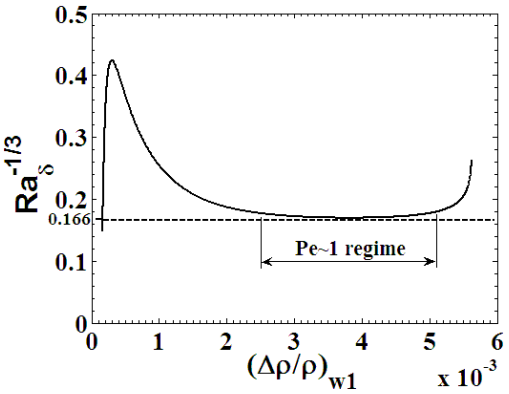

Fig.10: Variation of $Ra_\delta^{-1/3}$ based on the net flux q_d-q_u and ΔC_{w1}.

$$\frac{2}{E_1^{3/4}}\left(\frac{Sh}{Ra^{1/3}}\right)^{3/4} - D_1\frac{4Hl_m}{f\kappa}\left(\frac{ShSc}{Ra^2}\right)^{1/3} - 2D_3\frac{Ra_{wd}}{Ra} - 1 = 0, \qquad (16)$$

where $D_3=D_2e^{Pe}$ and Ra_{wd} is the Rayleigh number based on ΔC_{wd}. Here, E_1 is a function of ΔC in fig. 10, equal to 0.083 in the Pe~1 regime. Equation (16) has the correct asymptotes. When Pe$\rightarrow$0 in the diffusion regime, eq. (16) reduces to $Sh\sim Ra^{1/3}$. When $Ra_{wd}\rightarrow Ra$ and as $E_1= Ra_\delta^{-1/3} = Ra^{1/3}/Sh$, eq. (16) reduces to $Sh\sim Ra^2$. Figure 4 shows that the solution of eq. (16) for $2.43\text{x}10^{11} \le Ra \le 4.96\text{x}10^{11}$ (or $2.5\text{x}10^{-3} \le \Delta\rho/\rho \le 5.1\text{x}10^{-3}$) matches well with the experimental data in the Pe~1 regime. The flux scaling given by eq. (16) is a mixed scaling with the first term giving the diffusive scaling and the second term the advective scaling; the combined effects of these two scalings, captured by eq. (16), seems to scale as Sh~Ra to first order.

5. CONCLUSIONS

A new regime of convection across a permeable membrane is discovered when the flow is driven by the unstable density gradient due to a heavier brine layer above the membrane and a lighter water layer below it. This new regime is a transition regime between the

advection and the diffusion regimes. By using a coarser and thicker membrane compared to that of PA, we found that the flux (Sh) in this transition region scales approximately linearly with Rayleigh number (Ra), different from Sh~Ra^2 and Sh~$Ra^{1/3}$ scaling in the advection and the diffusion regimes. The near-membrane plumes had a weak alignment in this new regime compared to those in the advection regime. Based on this observation, the hypothesis that advection balances diffusion inside the membrane pore, is found to be true from Peclet number calculations, and hence this new regime is named as Pe~1 regime. Approximating a one dimensional convection-diffusion equation as the model for the flow in the membrane pore in the Pe~1 regime, the proposed phenomenology is able to explain the flux scaling Sh~Ra. Even though the magnitude of dimensionless flux is same as that of steady RBC, presence of advection velocities inside the membrane pore make the nature of the near-membrane boundary layers to be different from those of pure RBC.

APPENDIX

Calculation of ΔC_{wd}

ΔC_{wd} is approximated as a cubic polynomial satisfying the conditions

$\Delta C_{wd}=\Delta C_{adv}$ and $\frac{d}{\Delta C}(\Delta C_{wd})=1$
for $\Delta C =\Delta C_{adv}$ and (A1)

$\Delta C_{wd}=0$ and $\frac{d}{\Delta C}(\Delta C_{wd})=0$
for $\Delta C =\Delta C_{dif.}$ (A2)

Here, ΔC_{adv} =7.2g/l is the concentration difference at which the advection regime changes to the Pe~1 regime, and ΔC_{dif} =1g/l is the concentration difference at which the diffusion regime begins, as calculated from the 10g/l experiment in fig. 3. The final expression for ΔC_{wd} is

$$\Delta C_{wd} = \frac{(\Delta C-\Delta C_{dif})^2}{(\Delta C_{adv}-\Delta C_{dif})^3}\Big(2\Delta C_{adv}^2 - \Delta C\big(\Delta C_{adv}+\Delta C_{dif}\big)\Big). \quad \text{(A3)}$$

REFERENCES

1. Deardorff, J.W., 1970. Convective velocity and temperature scales for the unstable planetary boundary layer and for Rayleigh convection, Journal of the Atmospheric Sciences, 27:1211-1213.

2. Dworecki, K., Slezak, A., Ornal-Wasik, B., Wasik, S., 2005. Effect of hydrodynamic instabilities on solute transport in a membrane system, Journal of Membrane Science, 263:94-100.

3. Lide, D.R., 2003. CRC handbook of chemistry and physics, chapter 5, 84th edition, CRC press.

4. Puthenveettil, B. A., Arakeri, J.H., 2005. Plume structure in high Rayleigh-number convection. Journal of Fluid Mechanics, 542:217-249.

5. Puthenveettil, B.A., Arakeri, J.H., 2008. Convection due to an unstable density gradient across a permeable membrane, Journal of Fluid Mechanics, 609:139-170.

6. Slezak, A., Dworecki, K., Anderson, J.E., 1985. Gravitational effects on transmembrane flux: The Rayleigh-Taylor convective instability, Journal of Membrane Science, 23:71-81.

7. Rama Reddy, G.V., 2009. Investigations on convection across a horizontal permeable membrane, MS thesis, Indian Institute of Tecchnology Madras, Chennai, India.

8. Theerthan, S. A., Arakeri, J. H., 2000. Planform structure and heat transfer in turbulent free convection over horizontal surfaces, Physics of Fluids, 12:884-894.